Receiver-based compensation of transmitter-incurred nonlinear distortion in multiple-antenna OFDM systems

Tim C. W. Schenk*‡, Cédric Dehos°, Dominique Morche° and Erik R. Fledderus‡

* Philips Research Laboratories, High Tech Campus 37, 5656 AE Eindhoven, The Netherlands, tim.schenk@philips.com
° CEA-LETI MINATEC, 17 rue des Martyrs, 38 054 Grenoble CEDEX 9, France, cedric.dehos@cea.fr
‡ Eindhoven University of Technology, Radiocommunication Chair, PO Box 513, 5600 MB Eindhoven, The Netherlands

***Abstract*—To enable an efficient implementation of multiple-antenna OFDM systems, this paper proposes an approach to reduce the influence of transmitter-induced nonlinearities in such systems. The approach comprises a preamble design, an estimation method and a digital compensation algorithm. Correction for the nonlinearities of the different transmitter branches is applied in the receiver, which requires no extra hardware. A numerical performance evaluation shows that the proposed approach can successfully be applied with minimal performance degradation compared to non-impaired systems.**

I. Introduction

The combination of multiple-antenna techniques (MIMO) with OFDM is shown to be promising for application in next-generation high data rate wireless communication systems. Due to the high peak-to-average power ratio (PAPR) of OFDM signals, however, these systems are highly sensitive to nonlinearities in the system implementation, which can easily result in distortion and performance reduction. Nonlinearities will, consequently, form a major hurdle on the path to efficient and effective implementation of MIMO OFDM systems. We will here focus on the nonlinearities of the power amplifiers (PAs) in the transmitter (TX) front-ends, since these typically form the major sources of nonlinearity.

To overcome this problem, this paper proposes a method to efficiently reduce the impact of the TX nonlinearities in multicarrier MIMO systems. The proposed method corrects for the in-band distortion of the signals in the baseband part of the receiver (RX). As a result, highly nonlinear PAs, or a lower input power backoff to the PAs, can be applied and, consequently, the efficiency of the front-ends will be seriously improved. It is noted, however, that this approach can not deal with out-of-band spectral regrowth due to the nonlinearities. As such the PA efficiency will be mainly driven by the imposed emission mask.

In contrast to RX-based compensation, several promising approaches have been proposed in the last few years that digitally compensate for the TX nonlinearities in the TX baseband, i.e., digital predistortion, see e.g. [1]. Such approaches are promising for the downlink scenario, however, require extra hardware and processing at the TX side of the transmission link. In the uplink scenario, where the mobile station acts as TX, this might not be very advantageous due to increased cost and power consumption of the mobile terminal. For this scenario, RX-based compensation, as proposed in this paper, is promising, since no extra hardware is required and since most of the required processing is carried out in the base station.

Some methods for postdistortion for conventional OFDM systems have been proposed, e.g., [2], [3]. These approaches are not directly applicable to the regarded MIMO scenario, since all MIMO transmission chains will exhibit their own nonlinear transfer and MIMO detection is required. Furthermore, these approaches assume perfect channel and nonlinearity knowledge, which will not be available in a practical wireless system. Therefore this paper also proposes an estimation approach for both the MIMO wireless channel matrix and the multiple nonlinear responses.

The paper is organized as follows. First Section II introduces the system model. In Section III we propose a method to estimate both the linear and the nonlinear channel responses. Subsequently, we propose, based on these estimates, three compensation methods to remove the influence of nonlinearities in Section IV. Section V reports results from a simulation study to test the performance of the proposed approaches. Finally, conclusions are drawn in Section VI.

II. System Model

Consider a MIMO OFDM system with N_{T} TX and N_{R} RX antennas, denoted here as an $N_{\mathrm{T}}\times N_{\mathrm{R}}$ system, applying N_{C} subcarriers. Let us define the mth $N_{\mathrm{C}}N_{\mathrm{T}}\times 1$ MIMO OFDM vector to be transmitted in such a system to be given by $\mathbf{s}=\left[\mathbf{s}^T(0),\mathbf{s}^T(1),\ldots,\mathbf{s}^T(N_{\mathrm{C}}-1)\right]^T$, where $\mathbf{s}(k)$ denotes the $N_{\mathrm{T}}\times 1$ frequency-domain MIMO transmit vector for the kth subcarrier. The corresponding $N_{\mathrm{S}}N_{\mathrm{T}}\times 1$ time-domain signal vector, after applying the inverse discrete Fourier transform (IDFT) to $\mathbf{s}$ and adding a cyclic prefix (CP), is given by

$$\mathbf{u}=(\mathbf{\Theta}\mathbf{F}^{-1}\otimes\mathbf{I}_{N_{\mathrm{T}}})\mathbf{s}, \tag{1}$$

where $\otimes$ denotes the Kronecker product, $\mathbf{F}$ is the $N_{\mathrm{C}}\times N_{\mathrm{C}}$ Fourier matrix, the (i,k)th element of which equals $\exp(-j2\pi\frac{ik}{N_{\mathrm{C}}})$, and $\mathbf{I}_M$ represents the M-dimensional identity matrix. The addition of the CP of N_{G} samples is modeled by multiplication with matrix $\mathbf{\Theta}$, which adds the last N_{G} elements on top of the vector. The total symbol length thus equals $N_{\mathrm{S}}{=}N_{\mathrm{C}}{+}N_{\mathrm{G}}$. We assume that by design N_{G} is at least equal to the channel impulse response (CIR) length, preventing inter-symbol interference. The average total TX power is assumed to be equally divided among the TX antennas.

The regarded system experiences nonlinearities in the TX, modeled by N_{T}-dimensional nonlinearity $g(\cdot)$. Every TX branch will exhibit a different nonlinearity, i.e., the nonlinear function relating to the n_{T}th TX branch is denoted by $g_{n_{\mathrm{T}}}(\cdot)$. It is, subsequently, useful to define $\mathbf{u}_{n_{\mathrm{T}}}$ as the $N_{\mathrm{S}}\times 1$ subvector

1-4244-0264-6/07/$25.00 ©2007 IEEE

containing the elements of $\mathbf{u}$ relating to TX branch n_{T}. In a similar way we can define the $N_{\mathrm{C}}\times 1$ subvector $\mathbf{s}_{n_{\mathrm{T}}}$. The nonlinear distorted signal can then be written as $\mathbf{u}_{\mathrm{d}} = g(\mathbf{u})$, where the subvector for the n_{T}th TX branch is given by

$$\begin{aligned}\mathbf{u}_{\mathrm{d},n_{\mathrm{T}}} &= g_{n_{\mathrm{T}}}(\mathbf{u}_{n_{\mathrm{T}}}) = [u_{\mathrm{d},n_{\mathrm{T}}}(0),\ldots,u_{\mathrm{d},n_{\mathrm{T}}}(N_{\mathrm{s}}-1)]^T \\ &= [g_{n_{\mathrm{T}}}(u_{n_{\mathrm{T}}}(0)),\ldots,g_{n_{\mathrm{T}}}(u_{n_{\mathrm{T}}}(N_{\mathrm{s}}-1))]^T. \end{aligned} \quad (2)$$

The input to the nonlinearity is generally an amplitude and phase modulated bandpass signal, which in complex baseband representation is denoted by $u(n) = A(n)e^{j\phi(n)}$. The signal at the output of the nonlinearity $g(\cdot)$ is given by

$$u_{\mathrm{d}}(n) = g(u(n)) = g_{\mathrm{A}}(A(n))e^{j(\phi(n)+g_{\phi}(A(n)))}, \quad (3)$$

where $g_{\mathrm{A}}(\cdot)$ and $g_{\phi}(\cdot)$ model the amplitude-to-amplitude (AM-AM) and amplitude-to-phase (AM-PM) transfer, respectively.

The $N_{\mathrm{s}}N_{\mathrm{R}}\times 1$ received signal vector after transmission through the wireless MIMO channel, addition of RX noise and RX OFDM processing is given by

$$\begin{aligned}\mathbf{x} &= (\mathbf{F}\boldsymbol{\Upsilon}\otimes\mathbf{I}_{N_{\mathrm{R}}})(\mathbf{K}\mathbf{u}_{\mathrm{d}}+\mathbf{v}) = \mathbf{H}(\mathbf{F}\boldsymbol{\Upsilon}\otimes\mathbf{I}_{N_{\mathrm{T}}})\mathbf{u}_{\mathrm{d}}+\mathbf{n} \\ &= \mathbf{H}(\mathbf{F}\boldsymbol{\Upsilon}\otimes\mathbf{I}_{N_{\mathrm{T}}})g((\boldsymbol{\Theta}\mathbf{F}^{-1}\otimes\mathbf{I}_{N_{\mathrm{T}}})\mathbf{s})+\mathbf{n}, \end{aligned} \quad (4)$$

where $\mathbf{K}$ denotes the $N_{\mathrm{s}}N_{\mathrm{R}}\times N_{\mathrm{s}}N_{\mathrm{T}}$ CIR matrix, $\boldsymbol{\Upsilon}$ models the removal of the CP and $\mathbf{v}$ models the time-domain RX noise. The $N_{\mathrm{C}}N_{\mathrm{R}}\times N_{\mathrm{C}}N_{\mathrm{T}}$ block diagonal matrix $\mathbf{H}=(\mathbf{F}\boldsymbol{\Upsilon}\otimes\mathbf{I}_{N_{\mathrm{R}}})\mathbf{K}(\boldsymbol{\Theta}\mathbf{F}^{-1}\otimes\mathbf{I}_{N_{\mathrm{T}}})$ is the frequency domain version of $\mathbf{K}$ and $\mathbf{n}$ is the frequency domain version of $\mathbf{v}$.

For reasonable bandwidths, e.g. smaller than 20 MHz, we can reasonably assume that the nonlinearities are memoryless and (4) can be simplified to

$$\mathbf{x} = \mathbf{H}(\mathbf{F}\otimes\mathbf{I}_{N_{\mathrm{T}}})g((\mathbf{F}^{-1}\otimes\mathbf{I}_{N_{\mathrm{T}}})\mathbf{s})+\mathbf{n}. \quad (5)$$

Note that in a linear transmission chain (4) reduces to $\mathbf{x}=\mathbf{H}\mathbf{s}+\mathbf{n}$, which due to the block diagonal property of $\mathbf{H}$ preserves the orthogonality between the subcarriers.

III. MIMO Channel and Nonlinearities Estimation

To acquire reliable estimates of the transmitted data, we require estimates of the experienced (nonlinear MIMO) transfer. In the estimation hereof we will exploit that only N_{T} distinct nonlinearities occur, i.e., in the TX PAs, while $N_{\mathrm{T}}N_{\mathrm{R}}$ MIMO transfers per subcarrier have to be estimated. To that end, we propose the separation of the estimation of the nonlinear transfers and the linear MIMO channel. This is enabled by using a new frame format as depicted schematically in Fig. 1 for a two TX system. In this frame format the actual data transmission is preceded by a preamble consisting of pilot data used for the estimation of the linear MIMO channel and pilot data used for estimation of the TX-nonlinearities, indicated by "L train" and "NL train", respectively.

The estimation of the linear MIMO channel, the nonlinearities and their inverses, based on the presented preamble structure, is presented in Sections III-A, III-B and III-C, respectively.

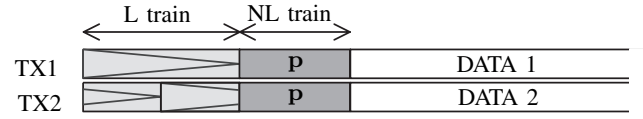

Fig. 1. Frame format for a 2 TX MIMO system enabling estimation of both the TX nonlinearities and the MIMO multipath channel.

A. Linear MIMO channel estimation

For the estimation of the MIMO multipath channel we propose the application of a constant modulus sequence. For the MIMO channel estimation we furthermore require the training sequences used on the different antennas to be orthogonal and shift orthogonal for at least the length of the channel. An efficient design can be achieved by the application of the Frank-Zadoff codes (FZC) [4] as training. The N^2-dimensional FZC is formed by a concatenation of the rows of the N-dimensional Fourier matrix. The preamble is formed by cyclicly shifting the code transmitted on the n_{T}th TX by $(n_{\mathrm{T}}-1)\lfloor N^2/N_{\mathrm{T}}\rfloor$ samples. Here we take the length of this preamble to be $N^2{=}N_{\mathrm{C}}$. The $N_{\mathrm{R}}N_{\mathrm{C}}\times 1$ received signal vector during the training for this $N_{\mathrm{T}}N_{\mathrm{C}}\times 1$ FZC-based preamble vector $\mathbf{u}_{\mathrm{p}}$ is given by

$$\begin{aligned}\mathbf{x}_{\mathrm{p}} &= (\mathbf{F}\boldsymbol{\Upsilon}\otimes\mathbf{I}_{N_{\mathrm{R}}})\mathbf{K}g((\boldsymbol{\Theta}\otimes\mathbf{I}_{N_{\mathrm{T}}})\mathbf{u}_{\mathrm{p}}) \\ &= (\mathbf{F}\boldsymbol{\Upsilon}\otimes\mathbf{I}_{N_{\mathrm{R}}})\mathbf{K}(\boldsymbol{\Theta}\otimes\mathbf{I}_{N_{\mathrm{T}}})(\mathbf{I}_{N_{\mathrm{C}}}\otimes\boldsymbol{\eta})\mathbf{u}_{\mathrm{p}}, \end{aligned} \quad (6)$$

where we used that we regard memoryless nonlinearities and that the training signal $\mathbf{u}_{\mathrm{p}}$ is constant modulus. Here $\boldsymbol{\eta}$ is an N_{T}-dimensional diagonal matrix defined as $\boldsymbol{\eta}=\mathrm{diag}\{\eta_1,\ldots,\eta_{N_{\mathrm{T}}}\}$. The nonlinear distorted signal vector corresponding to the n_{T}th TX branch is given by

$$g_{n_{\mathrm{T}}}(\mathbf{u}_{\mathrm{p},n_{\mathrm{T}}}) = \frac{g_{n_{\mathrm{T}}}(|\mathbf{u}_{\mathrm{p},n_{\mathrm{T}}}|)}{|\mathbf{u}_{\mathrm{p},n_{\mathrm{T}}}|}\mathbf{u}_{\mathrm{p},n_{\mathrm{T}}} = \eta_{n_{\mathrm{T}}}\mathbf{u}_{\mathrm{p},n_{\mathrm{T}}}, \quad (7)$$

where $|\mathbf{a}|$ denotes the vector of absolute values of the entries of $\mathbf{a}$. The complex parameter $\eta_{n_{\mathrm{T}}}$ thus models the amplitude change and phase shift of the constant modulus training sequence, induced by the AM-AM and AM-PM response of the nonlinearity of the n_{T}th branch, respectively. It is noted that for an AM-AM nonlinearity $\eta_{n_{\mathrm{T}}}$ is a real parameter.

It is, subsequently, readily found that least-squares estimation (LSE) of the MIMO channel estimation using $\mathbf{x}_{\mathrm{p}}$ yields $\hat{\mathbf{H}} = \mathbf{H}(\mathbf{I}_{N_{\mathrm{C}}}\otimes\boldsymbol{\eta})$, where we, for now, assumed a noiseless system. It can be conclude that the rows of $\hat{\mathbf{H}}$ corresponding to the n_{T}th TX differ by the complex factor $\eta_{n_{\mathrm{T}}}$ from the actual channel response $\mathbf{H}$.

B. Nonlinearity estimation

The second part of the preamble, as depicted in Fig. 1, must exhibit a PAPR behaviour similar to the data signal, to enable accurate estimation of the experienced nonlinear responses. Since the nonlinearities are estimated in the RX, i.e., after transmission through the frequency-selective fading channel, the signal must, moreover, exhibit some level of whiteness to avoid the total training sequence to coincide with a channel fade. To meet these requirements, a pseudo-random complex

white Gaussian signal is chosen with a variance equal to that of the signals in the data part. The same training is transmitted simultaneously from the different TX branches, yielding an overhead that is independent of the number of TX branches. The time-domain version of the $N_{\mathrm{c}}\times 1$ training vector is denoted by $\mathbf{p} = [p(1), \ldots, p(N_{\mathrm{c}})]^T$, to which a CP is added before transmission.

The resulting RX signal vector, after DFT processing, is found by

$$\mathbf{x} = \mathbf{H}(\mathbf{F}\boldsymbol{\Upsilon} \otimes \mathbf{I}_{N_{\mathrm{T}}}) g(\boldsymbol{\Theta}\mathbf{p} \otimes \mathbf{1}_{N_{\mathrm{T}}}) = \mathbf{H}\mathbf{q}_{\mathrm{d}}, \tag{8}$$

where $\mathbf{q}_{\mathrm{d}} = (\mathbf{F} \otimes \mathbf{I}_{N_{\mathrm{T}}}) g(\mathbf{p} \otimes \mathbf{1}_{N_{\mathrm{T}}})$ is the frequency-domain version of the nonlinear distorted training symbol and $\mathbf{1}_{N_{\mathrm{T}}}$ denotes the N_{T}-dimensional all-ones column vector. An estimate of $\mathbf{q}_{\mathrm{d}}$ can be found by applying zero-forcing MIMO processing using the estimated MIMO channel $\hat{\mathbf{H}}$, yielding

$$\hat{\mathbf{q}}_{\mathrm{d}} = \hat{\mathbf{H}}^{\dagger}\mathbf{x} = (\mathbf{I}_{N_{\mathrm{C}}} \otimes \boldsymbol{\eta})^{\dagger}\mathbf{H}^{\dagger}\mathbf{H}\mathbf{q}_{\mathrm{d}} = (\mathbf{I}_{N_{\mathrm{C}}} \otimes \boldsymbol{\eta}^{-1})\mathbf{q}_{\mathrm{d}}, \tag{9}$$

where † denotes the pseudo-inverse. If we then define the time-domain nonlinear distorted training signal, after removal of the CP, as $\mathbf{r}_{\mathrm{d}} = g(\mathbf{p} \otimes \mathbf{1}_{N_{\mathrm{T}}})$ its estimate is found using (9) by

$$\hat{\mathbf{r}}_{\mathrm{d}} \;=\; (\mathbf{F}^{-1} \otimes \mathbf{I}_{N_{\mathrm{T}}})\hat{\mathbf{q}}_{\mathrm{d}} = (\mathbf{I}_{N_{\mathrm{C}}} \otimes \boldsymbol{\eta}^{-1})\mathbf{r}_{\mathrm{d}}. \tag{10}$$

The estimated signal corresponding to the n_{T}th TX branch can then be written as

$$\hat{\mathbf{r}}_{\mathrm{d},n_{\mathrm{T}}} \;=\; \eta_{n_{\mathrm{T}}}^{-1}\mathbf{r}_{\mathrm{d},n_{\mathrm{T}}} = \eta_{n_{\mathrm{T}}}^{-1} g_{n_{\mathrm{T}}}(\mathbf{p}), \tag{11}$$

from which we conclude that the MIMO processing can successfully separate the different TX signals and this enables the estimation of the different nonlinear responses. To that end, we first consider LSE of the parameters of the polynomial model for the nonlinearity. In [5] it was shown that different nonlinear PA models, [6] and [7], can be mapped onto the polynomial model, making this a viable approach for the different modelled nonlinearities. Using the polynomial model, (11) can be rewritten for the nth sample as

$$\hat{r}_{\mathrm{d},n_{\mathrm{T}}}(n) = \eta_{n_{\mathrm{T}}}^{-1} p(n) \sum_{m=0}^{N-1} \beta_{m+1,n_{\mathrm{T}}} |p(n)|^m, \tag{12}$$

where $\beta_{m+1,n_{\mathrm{T}}}$ is the coefficient of the mth order of the polynomial nonlinearity for the n_{T}th TX branch.

Subsequently, we define $\boldsymbol{\beta}_{n_{\mathrm{T}}} = [\beta_{1,n_{\mathrm{T}}}\beta_{2,n_{\mathrm{T}}}, \ldots, \beta_{N,n_{\mathrm{T}}}]^T$ and $\boldsymbol{\Phi}$ to be the $N_{\mathrm{c}} \times N$ basis matrix, the (i,k)th element of which is given by $p(i)|p(i)|^{k-1}$. Note that $\boldsymbol{\Phi}$ is given by $\mathrm{diag}\{\mathbf{p}\}$ times the Vandermonde matrix of the amplitudes of the training vector values and $\boldsymbol{\beta}_{n_{\mathrm{T}}}$ contains the parameters of the Nth order polynomial model. Note, furthermore, that we can assume $\beta_{1,n_{\mathrm{T}}} = 1$ for all n_{T}, since the coefficient of the linear term is estimated as part of the MIMO CIR.

Using these expressions we can rewrite (12) in matrix notation as

$$\hat{\mathbf{r}}_{\mathrm{d},n_{\mathrm{T}}} = \eta_{n_{\mathrm{T}}}^{-1}\boldsymbol{\Phi}\boldsymbol{\beta}_{n_{\mathrm{T}}} = \boldsymbol{\Phi}\boldsymbol{\beta}'_{n_{\mathrm{T}}}, \tag{13}$$

where $\boldsymbol{\beta}'_{n_{\mathrm{T}}} = \eta_{n_{\mathrm{T}}}^{-1}\boldsymbol{\beta}_{n_{\mathrm{T}}}$. The LSE of the parameters of the polynomial nonlinearity model for the n_{T}th TX branch are then found by

$$\hat{\boldsymbol{\beta}}'_{n_{\mathrm{T}}} = \boldsymbol{\Phi}^{\dagger}\hat{\mathbf{r}}_{\mathrm{d},n_{\mathrm{T}}}. \tag{14}$$

The complexity of this solution can be reduced considerably by precalculating $\boldsymbol{\Phi}^{\dagger}$, which is possible since it is based on the known training vector $\mathbf{p}$.

When only odd orders occur in the nonlinearity, as for instance in [6], [7], the basis matrix $\boldsymbol{\Phi}$ can be simplified by omitting even orders. If we, moreover, assume a 5th order AM-AM nonlinearity, the basis $\boldsymbol{\Phi}$ reduces to a $N_{\mathrm{c}}\times 3$ matrix, the (i,k)th element of which is given by $p(i)|p(i)|^{2(k-1)}$ and $\boldsymbol{\beta}_{n_{\mathrm{T}}} = [1, \beta_{3,n_{\mathrm{T}}}, \beta_{5,n_{\mathrm{T}}}]^T$, where $\beta_{3,n_{\mathrm{T}}}$ and $\beta_{5,n_{\mathrm{T}}}$ are real parameters. Finally, for this nonlinearity the estimates of all parameters can be found from (14) as

$$\hat{\eta}_{n_{\mathrm{T}}} \;=\; \left(\hat{\beta}'_{n_{\mathrm{T}}}(1)\right)^{-1}, \tag{15}$$

$$\hat{\beta}_{3,n_{\mathrm{T}}} \;=\; \hat{\eta}_{n_{\mathrm{T}}}\hat{\beta}'_{n_{\mathrm{T}}}(2), \tag{16}$$

$$\hat{\beta}_{5,n_{\mathrm{T}}} \;=\; \hat{\eta}_{n_{\mathrm{T}}}\hat{\beta}'_{n_{\mathrm{T}}}(3), \tag{17}$$

where $\hat{\beta}'_{n_{\mathrm{T}}}(n)$ denotes the nth element of the estimated vector $\hat{\boldsymbol{\beta}}'_{n_{\mathrm{T}}}$. The estimate of the MIMO channel $\hat{\mathbf{H}}$ can be corrected for the constant amplitude error by using the estimate of (15).

A disadvantage of the polynomial basis is that the matrix $\boldsymbol{\Phi}^H\boldsymbol{\Phi}$ is often ill-conditioned for complex Gaussian signals and that, consequently, matrix inversion will incur numerical errors [8]. To overcome this problem, an *orthogonal polynomial basis* was derived using Gram-Schmidt orthonormalisation. Although this basis can be derived for the general problem of (13), we will here regard the specific problem where the nonlinearity can be modelled as a 5th order AM-AM nonlinearity. Since we only require the odd orders, the orthogonal polynomials are derived using the set of basis functions $\{A, A^3, A^5\}$, where $A(n) = |p(n)|$ denotes the amplitude of the elements of the training vector. The qth polynomial basis is denoted by $\psi_q(A)$ and the total set of orthonormal basis polynomials is given by

$$\psi_1(A) \;=\; A/\sqrt{\mu_2}, \tag{18}$$

$$\psi_2(A) \;=\; \alpha_1 A^3 + \alpha_2 A, \tag{19}$$

$$\psi_3(A) \;=\; (A^5 + \alpha_3 A^3 + \alpha_4 A)/\sqrt{\alpha_5}, \tag{20}$$

where we defined

$$\mu_q = \frac{1}{N_{\mathrm{c}}}\textstyle\sum_{q=1}^{N_{\mathrm{c}}} |p(n)|^q, \tag{21}$$

$$\alpha_1 = \sqrt{\mu_2/(\mu_2\mu_6 - \mu_4^2)}, \tag{22}$$

$$\alpha_2 = -\sqrt{\mu_4^2/(\mu_2^2\mu_6 - \mu_2\mu_4^2)}, \tag{23}$$

$$\alpha_3 = -(\mu_8\alpha_1 - \mu_6\alpha_2)\alpha_1, \tag{24}$$

$$\alpha_4 = (\mu_8\alpha_1 - \mu_6\alpha_2)\alpha_2 - \mu_6/\mu_2, \tag{25}$$

$$\alpha_5 = \mu_{10} + \alpha_3^2\mu_6 + \alpha_4^2\mu_2 + 2\alpha_3\mu_8 + 2\alpha_4\mu_6 + 2\alpha_3\alpha_4\mu_4. \tag{26}$$

For this orthonormal polynomial basis, the (i,k)th element of the $N_{\mathrm{c}}\times 3$ matrix $\boldsymbol{\Phi}$ is given by $\frac{p(i)}{|p(i)|}\psi_k(|p(i)|)$. The parameters of the nonlinearity can, similarly as for the other basis, be estimated using (14).

C. Inverse nonlinearity estimation

Instead of estimating the nonlinearity, as presented above, we can also directly estimate the inverse of the nonlinearity using the proposed preamble structure. This will show to be useful for the postdistortion procedure introduced in Section IV, since no inverse of the estimated nonlinearity has to be calculated. The polynomial estimation of the inverse nonlinearity is very similar to the estimation of the nonlinearity as presented in Section III-B. We first rewrite (11) as

$$\mathbf{p} = \ell_{n_\mathrm{T}}(\eta_{n_\mathrm{T}}\hat{\mathbf{r}}_{\mathrm{d},n_\mathrm{T}}) = \hat{\ell}_{n_\mathrm{T}}(\hat{\mathbf{r}}_{\mathrm{d},n_\mathrm{T}}), \tag{27}$$

where $\ell_{n_\mathrm{T}}(\cdot)$ denotes the inverse nonlinear function of $g_{n_\mathrm{T}}(\cdot)$, i.e., by definition $\ell_{n_\mathrm{T}}(g_{n_\mathrm{T}}(\mathbf{x})) = \mathbf{x}$. This is valid, since the transfer function of a PA is continuous and strictly monotonous and, thus, *bijective* with respect to the output range of the PA. Under the assumption that ℓ_{n_T} (or equivalently $\hat{\ell}_{n_\mathrm{T}}$) can be modelled by a polynomial model of order N, (27) can be rewritten in matrix notation, yielding $\mathbf{p} = \mathbf{\Phi}_{n_\mathrm{T}}\boldsymbol{\chi}_{n_\mathrm{T}}$. Here we defined $\boldsymbol{\chi}_{n_\mathrm{T}}=[\chi_{1,n_\mathrm{T}}, \chi_{2,n_\mathrm{T}}, \ldots, \chi_{N,n_\mathrm{T}}]^T$ and the (i,k)th element of the $N_\mathrm{C}\times N$ matrix $\mathbf{\Phi}_{n_\mathrm{T}}$ is given by $\hat{r}_{\mathrm{d},n_\mathrm{T}}(i)|\hat{r}_{\mathrm{d},n_\mathrm{T}}(i)|^{k-1}$.

The LSE of the parameters of the polynomial model are then given for the n_Tth TX branch as

$$\hat{\boldsymbol{\chi}}_{n_\mathrm{T}} = \mathbf{\Phi}^{\dagger}_{n_\mathrm{T}}\mathbf{p}. \tag{28}$$

It is noted that also here orthogonal bases can be applied. The problem is, however, that $\mathbf{\Phi}_{n_\mathrm{T}}$ is here dependent on $\hat{\mathbf{r}}_\mathrm{d}$. Therefore, the parameters of the orthonormal basis have to be calculated for every realisation. Alternatively, a basis could be derived based on the distribution of $\mathbf{r}_\mathrm{d}$, as in [8].

Note that additionally, in contrast to the method presented in Section III-B, the inverse of $\mathbf{\Phi}$ can not be precalculated, since it contains the estimates of the nonlinearly distorted TX signals. Furthermore, it has to be calculated separately for every TX branch. This will result in a higher complexity in the estimation phase, but will be shown to enable a postdistortion implementation of lower complexity.

IV. Digital RX-based compensation

We will regard three methods of digital compensation here, which are all based on the estimates obtained from the algorithms proposed in Section III. For all methods, first an estimate of the nonlinear distorted TX vector is applied using the channel estimate $\hat{\mathbf{H}}$, yielding $\hat{\mathbf{u}}$.

The first two proposed algorithms are based on postdistortion. For the first one, we use the estimates of the parameters of the inverse nonlinearity of Section III-C to find the postdistorted signal corresponding to the n_Tth TX stream, which is given by

$$\hat{u}'_{n_\mathrm{T}}(n) = \hat{u}_{n_\mathrm{T}}(n)\sum_{m=0}^{N-1}\hat{\chi}_{m+1,n_\mathrm{T}}|\hat{u}_{n_\mathrm{T}}(n)|^m \ . \tag{29}$$

The second method that we propose applies the estimates of the nonlinearities found from Section III-B. The data is now found by applying Lagrange interpolation on the data. The AM-AM postdistorted signal for this method is given by

$$\hat{u}'_{n_\mathrm{T}}(n) = \frac{\hat{u}_{n_\mathrm{T}}(n)}{|\hat{u}_{n_\mathrm{T}}(n)|}\sum_{m=1}^{M}a(m)\prod_{l=1,m\neq l}^{M}\frac{|\hat{u}_{n_\mathrm{T}}(n)| - b_{n_\mathrm{T}}(l)}{b_{n_\mathrm{T}}(m) - b_{n_\mathrm{T}}(l)} \ , \tag{30}$$

where $a(m)$ is the M-dimensional basis used for the Lagrange interpolation, which is chosen in a tradeoff between the quality of fit and smoothness of the output signal. The points used for the interpolation are found using the estimated nonlinear function $\hat{g}(\cdot)$ and given by $b_{n_\mathrm{T}}(m) = \hat{g}_{n_\mathrm{T}}(a(m))$. The choice of the basis $a(m)$ is elaborated on in [9].

The third algorithm is based on the iterative distortion removal (IDR) method proposed in [2] and [3], where the distortion caused by the nonlinearities is estimated using a decision directed approach. First initial estimates of the data are calculated, which are then used together with estimates of the nonlinearities from Section III-B to derive estimates of the distortion term. This distortion term is then subtracted from the original signal output of the MIMO processing and again detection is applied. This process can be repeated several times to improve performance.

V. Numerical Results

To evaluate the performance of the proposed estimation and compensation techniques, Monte Carlo simulations were performed. As a test-case a MIMO extension of the IEEE 802.11a standard was chosen. All TX branches are simulated to experience the solid-state amplifier model of [7] with p=1 and A_0=3, corresponding to highly nonlinear PAs with good efficiency and only odd orders. The nonlinearities are separately estimated for the different branches. The length of the training symbols is equal to the length of an OFDM symbol. One symbol is used for the estimation of the MIMO channel and one for the estimation of the nonlinearities. The channel is modelled as a spatially uncorrelated Rayleigh faded MIMO channel with a rms delay spread of 50 ns.

As a first performance measure we regard the MSE in the estimated signals using the estimated nonlinearities and inverse nonlinearities. We compare three MSEs in the following, which are defined as

- MSE of the nonlinear distorted signal: $\mathrm{MSE}_1 = \mathbb{E}\left[|\hat{u}_{\mathrm{d},n_\mathrm{T}}(n) - u_{n_\mathrm{T}}(n)|^2\right]$, where $\hat{\mathbf{u}}_\mathrm{d} = (\mathbf{F}\mathbf{\Upsilon}\otimes\mathbf{I}_{N_\mathrm{r}})\hat{\mathbf{H}}^{\dagger}\mathbf{x}$ for a system that does experience the nonlinearities.
- MSE of the postdistorted signal using the *estimated inverse nonlinearities*: $\mathrm{MSE}_2 = \mathbb{E}\left[|\hat{u}'_{n_\mathrm{T}}(n) - u_{n_\mathrm{T}}(n)|^2\right]$, where $\hat{u}'_{n_\mathrm{T}}(n)$ is found using (29).
- MSE of the distorted signal using the *estimated nonlinearities*: $\mathrm{MSE}_3 = \mathbb{E}\left[|\hat{g}_{n_\mathrm{T}}(\hat{u}_{n_\mathrm{T},\mathrm{lin}}(n)) - u_{\mathrm{d},n_\mathrm{T}}(n)|^2\right]$, where $\hat{\mathbf{u}}_\mathrm{lin} = (\mathbf{F}\mathbf{\Upsilon}\otimes\mathbf{I}_{N_\mathrm{r}})\hat{\mathbf{H}}^{\dagger}\mathbf{x}$ for a linear system.

Figure 2 compares the MSE performance for a system with perfect channel knowledge (in dashed lines) with that of a system using an estimated MIMO channel (in solid lines) found using the method of Section III-A, for a 16-QAM 2×4 system.

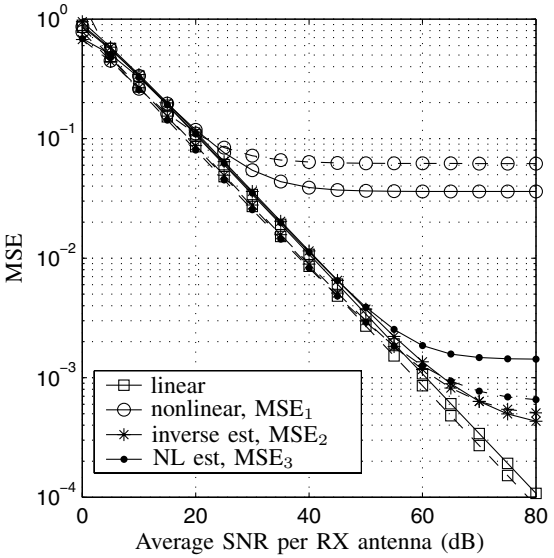

Fig. 2. MSE for a 2×4 system with perfect (dashed lines) and estimated (solid lines) MIMO wireless channel knowledge.

We conclude that the MSE degradation for low SNR is equal to that of the reference curve (linear). Interestingly, the MSE performance of the uncorrected nonlinearity (MSE_1) improves for the estimated MIMO channel for high SNR values, compared to the case of perfect channel knowledge. This is explained by the fact that the estimated channel is scaled by a factor η_{n_T}, which partly corrects for the scaling of the signal by the nonlinearities. The MSE performance for the estimated inverse nonlinearities, MSE_2, is almost equal for the estimated and perfect channel knowledge case, while a small MSE degradation is observed for MSE_3. This can be explained by the fact that the first order now also has to be estimated due to unknown scaling of the linear MIMO channel estimate.

To test the performance of the combined estimation/compensation approach, bit-error rate (BER) simulations were carried out, the results of which are depicted in Fig. 3. Results are depicted for a 2×4 system applying 64-QAM modulation and no coding. The BER results of a system not experiencing nonlinearities ("linear") and experiencing nonlinearities, but not applying correction ("nonlinear") are given as reference in the figure. The Lagrange-based postdistortion (PD) results are given for a linear basis with M=5. The results for a system applying IDR are given for the first three iterations.

We can conclude that severe BER degradation occurs due to the introduced nonlinearities; flooring occurs at a level of $7 \cdot 10^{-3}$. PD using either the estimated inverse nonlinearities or the estimated nonlinearities and Lagrange interpolation can successfully reduce the influence of the nonlinearities. The resulting BER curves are shifted 0.5 dB compared to that of a system not experiencing nonlinearities. It is noted that the Lagrange-based postdistortion performs a little worse than the other postdistortion method for low SNR values. The IDR method already improves the BER performance in the initial iteration, which is further improved in the following iterations. At a BER of 10^{-4}, a degradation of 2 dB compared to the ideal

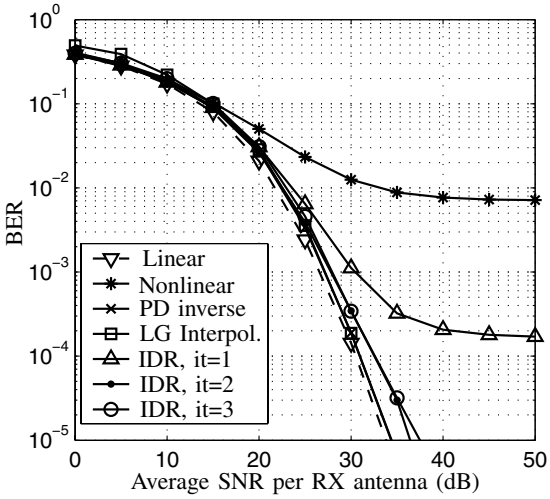

Fig. 3. BER results for a 2×4 64-QAM system applying different RX-based nonlinearity correction methods.

performance is achieved. When more iterations are applied, no further performance improvement is observed. The algorithms will reveal similar gains for coded MIMO OFDM systems.

VI. Conclusions

A novel approach to considerably reduce the performance impact of transmitter-induced nonlinearities in multiple-antenna OFDM system has been proposed in this paper. Digital compensation for the nonlinearities of the different transmitter branches is applied in the receiver, which requires no extra hardware. The approach comprises a preamble design, different estimation algorithms and several digital compensation methods. From a numerical study it is concluded that the combined estimation and compensation approach can considerably reduce the performance impact of the nonlinearities. As such, the PA efficiency is mainly driven by the nonlinearity-caused spectral regrowth and the emission mask.

References

[1] H. W. Kang, Y. S. Cho, and D. H. Youn, "On compensating nonlinear distortions of an OFDM system using an efficient adaptive predistorter," *IEEE Trans. on Commun.*, vol. 47, pp. 522–526, April 1999.

[2] H. Chen and A. M. Haimovich, "Iterative estimation and cancellation of clipping noise for OFDM signals," *IEEE Commun. Letters*, vol. 7, pp. 305–307, July 2003.

[3] J. Tellado, L. M. C. Hoo, and J. M. Cioffi, "Maximum-likelihood detection of nonlinearly distorted multicarrier symbols by iterative decoding," *IEEE Trans. on Commun.*, vol. 51, pp. 218–228, Feb. 2003.

[4] R. Frank and S. Zadoff, "Phase shift pulse codes with good periodic correlation properties," *IRE Trans. on Inf. Theory*, pp. 381–382, 1962.

[5] T. C. W. Schenk, P. F. M. Smulders, and E. R. Fledderus, "Impact of nonlinearities in multiple-antenna OFDM transceivers," in *Proc. SCVT2006, Liege, Belgium*, Nov. 2006, pp. 53–56.

[6] A. A. M. Saleh, "Frequency-independent and frequency-dependent nonlinear models of TWT amplifiers," *IEEE Trans. on Commun.*, vol. COM-29, pp. 1715–1720, Nov. 1981.

[7] C. Rapp, "Effects of HPA-nonlinearities on a 4-DPSK/OFDM-signal for a digital sound broadcasting system," in *Proc. second European conf. on Satellite Commun., Liege, Belgium*, Oct. 1991, pp. 179–184.

[8] R. Raich and G. T. Zhou, "Orthogonal polynomials for complex Gaussian processes," *IEEE Trans. on Sign. Proc.*, Oct. 2004.

[9] T. C. W. Schenk, *RF Impairments in Multiple Antenna OFDM: influence and mitigation*, Ph.D. thesis, Eindhoven University of Technology, Nov. 2006.